TSUNAMI HAZARD ANALYSIS OF LAND USE IN KARANGKANDRI VILLAGE, CILACAP, CENTRAL JAVA

(Analisis Bahaya Tsunami Terhadap Tata Guna Lahan di Desa Karangkandri, Cilacap, Jawa Tengah)

Yeriko Septiawan[1], Robet Triarjunet [1,2], Osmar Shalih[3]
[1]Amcolabora Institute
[2]Master's Program in Geography, Faculty of Geography, Universitas Gajah Mada
[3]National Disaster Management Authority
Ruko Anggrek Grand Depok City, Jl. Boulevard Grand Depok City No.C1 No 36, Tirtajaya, Kec. Sukmajaya, Kota Depok, Jawa Barat 16421
E-mail: yerico.septiawan@amcolabora.or.id

Diterima: 4 Januari 2025; Direvisi: 25 Maret 2025; Disetujui untuk Dipublikasikan: 19 Mei 2025

ABSTRACT

Indonesia is located in the Ring of Fire, making it highly vulnerable to natural disasters such as earthquakes and tsunamis. Karangkandri Village in Cilacap Regency, situated along the southern coast of Java, is at high risk due to the subduction activity of the Indo-Australian and Eurasian plates. Most of the village consists of residential and agricultural areas that are highly susceptible to tsunami impacts. This study aims to map tsunami hazard zones, analyze their impact on land use, and provide policy recommendations for disaster mitigation. The research employs the COMCOT v1.7/1.7b numerical model to simulate tsunami propagation and inundation, utilizing topography, bathymetry, and land use data as inputs. The tsunami hazard index is calculated using a fuzzy logic method to classify hazard levels into low, medium, and high. The simulation results indicate that the tsunami will reach Karangkandri Village within 54 minutes, with a maximum wave height of 7.34 meters, affecting a total of 416.11 hectares of the village, of which 339.99 hectares are classified as high hazard. The most significantly impacted land uses are residential yards (127.59 hectares) and rice fields (101.87 hectares). This study provides a foundation for the government to formulate disaster mitigation policies, such as constructing tsunami-resistant infrastructure, enhancing early warning systems, and promoting community education. Policy recommendations include establishing local tsunami monitoring posts and developing effective evacuation routes. The government should integrate these findings into regional spatial planning and disaster mitigation programs, while also enhancing community capacity through training and evacuation drills to reduce tsunami disaster risks.

Keywords: Cilacap, Fuzzy, Karangkandri, Land use, Numerical Model, Propagation, Tsunami

ABSTRAK

Indonesia terletak di wilayah *Ring of Fire* yang mengakibatkan rentan terhadap bencana alam seperti gempa bumi dan tsunami, Desa Karangkandri yang berada di Kabupaten Cilacap merupakan daerah pesisir selatan Jawa yang berisiko tinggi akibat aktivitas subduksi lempeng Indo-Australia dan Eurasia, sebagian besar wilayah Desa Karangkandri merupakan permukiman dan lahan pertanian yang rentan terhadap dampak tsunami. Penelitian ini bertujuan untuk memetakan zona bahaya tsunami, menganalisis dampaknya terhadap penggunaan lahan, dan memberikan rekomendasi kebijakan mitigasi bencana. Metode yang digunakan adalah model numerik COMCOT v1.7/1.7b untuk simulasi propagasi dan inundasi tsunami, dengan data topografi, batimetri, dan penggunaan lahan sebagai input. Indeks bahaya tsunami dihitung menggunakan metode logika fuzzy untuk mengklasifikasikan tingkat bahaya menjadi rendah, sedang, dan tinggi. Hasil simulasi menunjukkan bahwa tsunami akan mencapai Desa Karangkandri dalam waktu 54 menit dengan ketinggian maksimum 7,34 meter, di mana 416,11 hektar wilayah desa terdampak tsunami, dengan 339,99 hektar termasuk dalam kategori bahaya tinggi. Penggunaan lahan yang paling terdampak adalah pekarangan (127,59 hektar) dan sawah (101,87 hektar). Penelitian ini memberikan dasar bagi pemerintah dalam merumuskan kebijakan mitigasi bencana, seperti pembangunan infrastruktur tahan tsunami, peningkatan sistem peringatan dini, dan edukasi masyarakat. Rekomendasi kebijakan termasuk pembangunan pos pemantauan tsunami lokal dan penyediaan rute evakuasi yang efektif. Pemerintah perlu mengintegrasikan hasil penelitian ini ke dalam rencana tata ruang wilayah dan program mitigasi bencana, serta meningkatkan kapasitas masyarakat melalui pelatihan dan simulasi evakuasi untuk mengurangi risiko bencana tsunami.

Kata Kunci: Cilacap, Fuzzy, Karangkandri, Penggunaan lahan, Numerical Model, Penjalaran, Tsunami

INTRODUCTION

Geographically, Indonesia is bordered by the Indo-Australian plate, the Eurasian plate, and the Pacific plate, all of which are major tectonic plates of the world, known as the Ring of Fire or the Circum-Pacific Belt. This condition exposes Indonesia to potential natural disasters such as volcanic eruptions, earthquakes, landslides, and tsunamis (BNPB, 2023). Historically, tsunamis have claimed the lives of approximately 280,000 people across 14 countries, particularly in Asian countries, including Indonesia. Tsunamis are among the deadliest natural disasters in history (Law & Pangka, 2014; Sabah & Sil, 2023). Tsunamis in Indonesia are caused by megathrust earthquakes occurring in subduction zones at the intersection of tectonic plates. Areas bordering the sea and traversed by megathrust zones will experience severe social, economic, and environmental impacts in the event of a tsunami disaster (Yusup et al., 2023). Tsunami hazard mitigation requires a comprehensive and systematic approach with various preventive measures, including vegetation-based mitigation such as mangrove cultivation and coral reefs (Chen et al., 2024; Van Balen et al., 2024).

The southern coastal region of Java Island is one of the areas with a high probability of earthquakes and tsunamis due to its direct proximity to the Indo-Australian plate boundary (Amri et al., 2017). According to the earthquake map for Java from 2009-2023 (BMKG, 2024), 80% of the earthquake epicenters are located offshore of southern Java, with the remaining 20% on the mainland and offshore northern Java. Earthquakes centered offshore southern Java generally occur due to the asymmetrical subduction activity between the Indo-Australian Oceanic and Eurasian Continental Plates.

Historical records show that Cilacap Regency was affected by a tsunami during the Pangandaran tsunami in 2006. This earthquake resulted from thrust-fault activity at the boundary between the two tectonic plates, producing tsunami waves 3-5 meters high. Consistent with studies on Probabilistic Tsunami Hazard Analysis (PTHA) (BNPB, 2019), Cilacap Regency has the potential for recurring tsunamis with a height of 5.4 meters in a 100-year return period, 10.6 meters in a 500-year return period, and 29.1 meters in a 2500-year return period (BNPB, 2023).

Administratively, Karangkandri Village is located in Kesugihan Subdistrict, Cilacap Regency, Central Java Province. Geographically, it is a coastal area with the Cilacap PLTU industrial zone and fishermen housing, directly bordering the Indo-Australian subduction zone along the southern coast of Java, which is prone to tsunamis. Therefore, the local government has formulated a policy through the Cilacap Regency Spatial Plan, designating Karangkandri Village as an area traversed by the disaster evacuation network (Pemerintah Cilacap, 2021).

Given the history of disaster events, it is necessary to map the tsunami hazard zone to identify tsunami sources and arrival times and determine the tsunami inundation hazard index (Aranguiz et al., 2024; Setyaningsih et al., 2023), which can also be used to assess its impact on land use in Karangkandri Village. This research is expected to serve as a basis for government consideration in determining the location and path of disaster evacuation in formulating regional policies such as spatial and mitigation planning.

METHODS

Study Area

Karangkandri Village is one of the 16 villages in Kesugihan Subdistrict, Cilacap Regency. The population of Karangkandri Village is 8,461 people (Central Bureau of Statistics, 2023). Land use is predominantly residential with a uniformly distributed pattern. Geographically, Karangkandri Village is a lowland area with agricultural potential, and its southern region directly borders the Indian Ocean. Karangkandri Village has abundant fishing potential but is also threatened by tsunamis. Almost all residential areas are near the coast. Karangkandri Village is one of the areas prone to tsunami disasters. The total area of Karangkandri Village is 420.55 hectare (**Figure 1**).

Method

This tsunami hazard study is an evaluation of natural processes that have the potential to become sources of tsunami disasters for human life. The tsunami hazard analysis activities are carried out by considering several aspects. The tsunami source is from the National Center for Earthquake Studies (PuSGeN). The tsunami propagation and inundation model in Karangkandri Village is conducted using a numerical model. Determination of the parameters from the characteristics of the tsunami source at the geographical location. Calculation of the tsunami hazard index level concerning land use in the surrounding area using fuzzy logic classification (BNPB, 2019).

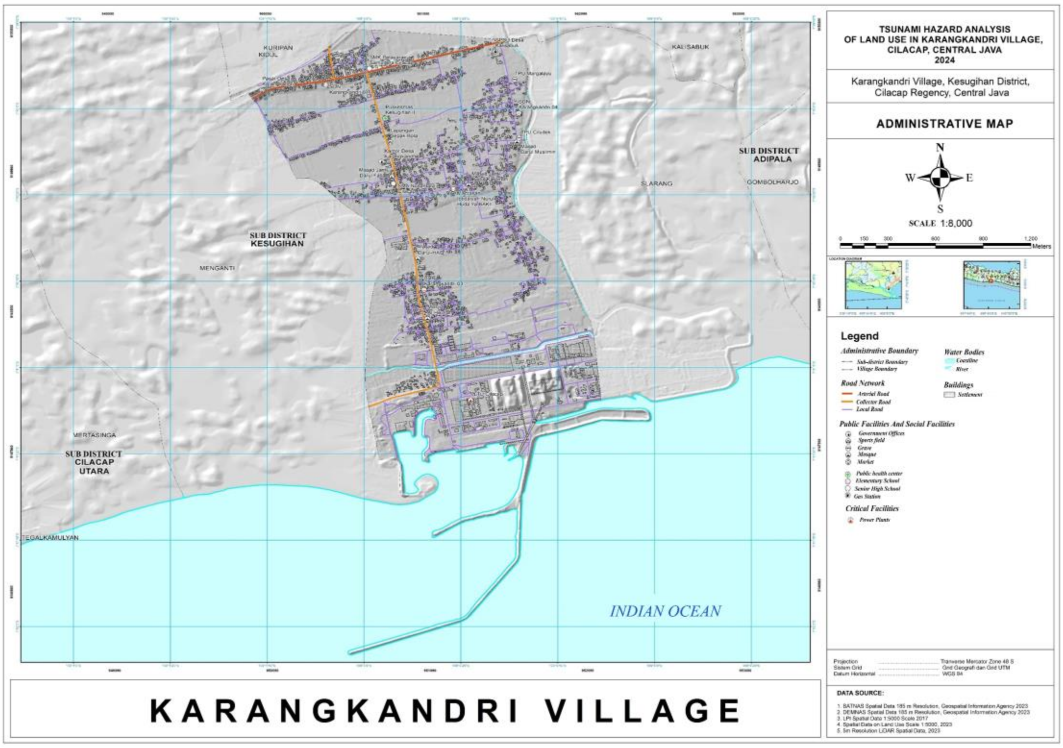

Figure 1. Administrative map of Karangkandri Village.

Numerical Model of Tsunami Propagation and Inundation

A numerical model is a technique used to formulate mathematical problems so that they can be solved with computational/arithmetic operations. The software used to model tsunami propagation and inundation initially involved physical laboratory experiments, which were then transformed into numerical test models using Cornell Multigrid Coupled Tsunami (COMCOT) methods (Zuliansah et al., 2023). This study uses COMCOT v1.7/1.7b, developed by (Xiaoming Wang & Liu, 2009), which is designed to simulate the impact of tsunami waves on the study area with grid resolution visualization models. COMCOT uses the Shallow Water Equations in a nonlinear form to describe tsunami wave propagation. The Coriolis effect in these equations causes the deviation of water mass movement to the right in the Northern Hemisphere and to the left in the Southern Hemisphere. The general form of **Equations 1** is (Zuliansah et al., 2023):

$$\frac{\partial d}{\partial t} + \left\{\frac{\partial P}{\partial x} + \frac{\partial Q}{\partial y}\right\} = -\frac{\partial d}{\partial t}$$
$$\frac{\partial P}{\partial t} + \frac{\partial}{\partial x}\left\{\frac{P^2}{H}\right\} + \frac{\partial}{\partial y}\left\{\frac{PQ}{H}\right\} + gH\frac{\partial \eta}{\partial x} + F_x = 0$$
$$\frac{\partial Q}{\partial t} + \frac{\partial}{\partial x}\left\{\frac{PQ}{H}\right\} + \frac{\partial}{\partial y}\left\{\frac{Q^2}{H}\right\} + gH\frac{\partial \eta}{\partial Y} + F_Y = 0 \text{............} \textbf{(1)}$$

While η represents the elevation of the water surface (m), t denotes the passage of time in seconds (s). Additionally, d refers to the water depth (m), while P and Q indicate the momentum fluxes in the horizontal (x) and vertical (y) directions, measured in cubic meters per second (m³/s).

The coefficient f represents the Coriolis force factor, which depends on latitude and is given by the **Equation 2**.

$$F = 2\Omega \sin\phi \text{ ....} \textbf{(2)}$$

Where Ω is the Earth's rotational speed, and ϕ is the latitude. The Coriolis force influences large-scale fluid motion, causing water mass movement to deviate to the right in the Northern Hemisphere and to the left in the Southern Hemisphere.

Meanwhile, H represents the total water depth (m), which is a combination of the static water depth and the elevation of the water surface due to waves. Bottom friction forces also play a role in water movement dynamics, represented by F_x and F_y which indicate the bottom friction forces in the horizontal (x) and vertical (y) directions, respectively.

The simulation of tsunami propagation and inundation follows the stages of the numerical simulation process, which are part of the tsunami hazard assessment process flowchart. The propagation simulation begins using domain design data inputs, bathymetry, and topography. (Crescenzo et al., 2024). The inundation simulation on land areas uses the results of the propagation simulation, supplemented with surface roughness coefficient data obtained from land use maps (Aljber et al., 2024; Briseid Storrøsten et al., 2024). The propagation and inundation modeling results are used to obtain data on tsunami run-up, height, and arrival time (Koshimura et al., 2024; Matsutomi & Arikawa, 2023).

This numerical tsunami simulation applies the Nested Grid concept, wherein a high-resolution grid is embedded within a domain with a lower-resolution grid (**Figure 2**). This concept is advantageous for optimizing computational time using computational domains and bathymetry depth contours (Yamazaki et al., 2011). The benefit of this method is that it requires detailed grids only for the study area, which speeds up the simulation time while minimizing numerical errors (Hayashi et al., 2018).

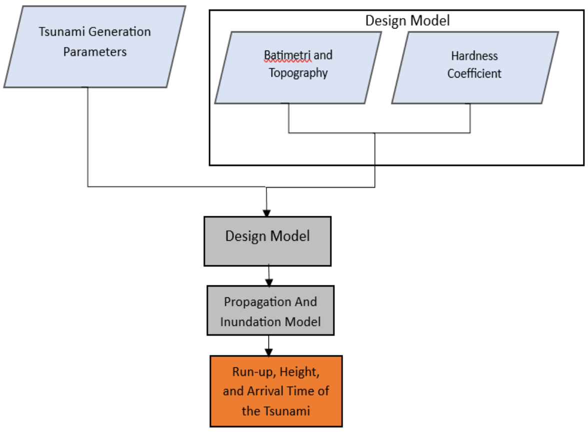

Source: Modified flowchart from the user manual for Comcot Version 1.7, 2023

Figure 2. Flowchart of numerical simulation process for Tsunami propagation and inundation.

Fuzzy Logic Method.

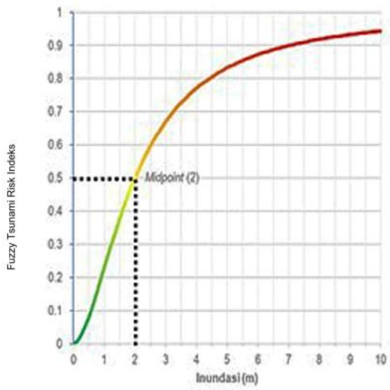

undasi (m)	Tsunami Risk Index	Class
10.00	0.944	High
9.00	0.933	High
8.00	0.9	High
7.00	0.872	High
6.00	0.833	High
5.00	0.771	High
4.00	0.687	High
3.50	0.636	Medium
3.00	0.596	Medium
2.75	0.554	Medium
2.50	0.500	Medium
2.25	0.442	Medium
2.00	0.305	Low
1.50	0.229	Low
1.00	0.152	Low
0.50	0.081	Low
0.25	0.026	Low
0.00	0.000	Low

Source: (BNPB, 2018)

Figure 3. Methodology for determining hazard index using fuzzy membership approach.

The tsunami hazard index indicates the transformation value of tsunami height estimates, represented numerically within a range of 0 to 1. If the tsunami height increases (more than 3 meters), the index value approaches 1. Conversely, if the tsunami height exceeds 1 meter, the index value approaches 0. This transformation utilizes a fuzzy logic approach, as illustrated in **Figure 3** (BNPB, 2018). The general form of these **Equations 3** (BNPB, 2012) is:

$$H_{loss} = \left(\frac{167\,n^2}{H_0^{1/3}}\right) + 5 \sin S \text{..} \textbf{(3)}$$

Where:

H_{loss} :tsunami wave height loss per 1 m of inundation distance

n :surface roughness coefficient

H_0 :tsunami wave height at the shoreline (m)

S :surface slope angle (degrees)

The results of tsunami inundation depth are transformed from meters to hazard indices and categorized, as shown in **Table 1**. Based on the classifications in that table, the exposed area can be grouped into three classes: low, medium, and high (BNPB, 2018). This grouping is based on tsunami height data resulting from propagation analysis and tsunami inundation.

Table 1. Range of Inundation and Hazard Index base don Hazard Classes

Classification	Inundation (meter)	Indeks
Low	≤ 1	0 – 0,333
Medium	1 < Inundation ≤ 3	0,334 – 0,666
High	> 3	0,667 - 1

Source: (BNPB, 2018)

Table 2. Data used in this study.

No	Type of Data	Resolution /Scale	Source	Year
1	BATNAS Spatial Data	185 m	Geospatial Agency	2023
2	DEMNAS Spatial Data	185 m	Geospatial Agency	2023
3	LPI Spatial Data	1:5000	Geospatial Agency	2017
4	Spatial Data on Land Use	1:5000	Geospatial Agency	2023
5	LiDAR Spatial Data	5 m	Geospatial Agency	2023

The spatial data mentioned above **(Table 2)** is essential as it plays a crucial role in tsunami risk analysis, primarily in understanding the tsunami hazard's impact on the population, buildings, and land use in the coastal area of Karang Kandri Village.

Results And Discussion

Tsunami Generation Source

Karangkandri Village is located on the southern coast of Java Island, characterized by a low-lying coastal plain with gentle geomorphological features. Although not all coastal villages are automatically prone to tsunamis due to the influence of elevation and coastal morphology such as the presence of steep cliffs in some areas Karangkandri Village is considered highly vulnerable because it is characterized by low-lying topography, which makes it particularly susceptible to tsunami inundation. This geographical condition, combined with its proximity to the Indo-Australian subduction zone, makes the village highly vulnerable to tsunami hazards. Earthquakes originating off the southern coast of Java are typically caused by activity between the Indian - Australian Oceanic Tectonic Plate and the Eurasian Continental Plate. The Sunda Arc tsunami disaster is highly likely to occur in the offshore western Sumatra region and the southern coast of Java (Prasetyo et al., 2023). Tsunami disasters in these areas are generally caused by the dynamics of large-scale uplift fault movements (megathrust) within oblique and frontal thrust systems between the Indian - Australian Oceanic Tectonic Plate and the Eurasian Continental Plate. Based on the geometry and dimensions of the thrust zone, the distribution density of epicentres and hypocenters, focal mechanisms, and the history of tsunamigenic earthquakes, the Outer Arc Ridge Zone, where the Sunda Arc's megathrust uplift faults are located, can be divided into 11 segments (Handoyo et al., 2023). The southern coast of Java is highly vulnerable to tsunamis due to its geological conditions, low elevation, and history of destructive events.

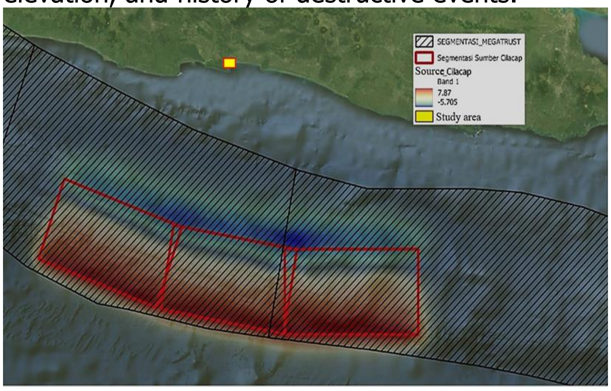

Source: (PuSGeN, 2017)

Figure 4. Source of Tsunami Generation in Karangkandri Village, Cilacap Regency.

The selection of earthquake sources triggering tsunamis in the Cilacap Regency area, particularly in the village of Karangkandri, is based on earthquakes occurring in the megathrust zone with a magnitude of 8.8 Mw, which represents the worst-case earthquake scenario potentially occurring in Cilacap Regency. Based on historical records, there have been at least two tsunami incidents associated with the megathrust zone in the Central Java segment: the Banyuwangi tsunami in 1994 with a magnitude of 7.6 Mw and the Pangandaran tsunami in 2006 with a magnitude of 7.8 Mw. (Pusgen, 2017) The likelihood of a megathrust earthquake source located in the southern part significantly influences the earthquake hazard level in Cilacap and its surrounding areas compared to other earthquake sources on land (Ridwan et al., 2023). This megathrust segment is sufficiently close to the study area and has a considerable maximum magnitude potential, thus capable of producing more muscular tremors.

The parameters used in the numerical simulation of tsunami generation for the Indo-Australian Subduction Source can be seen in Table 2. This subduction source has three fault segments with a length of 14.1 km, fault width of 91 km, earthquake depth of 14-18 km, dip angle of 11-17 degrees, and a Rake Angle of 90 degrees. The strike value varies for each segment, following the fault line/direction pattern in each segment.

Figure 4 illustrates the earthquake source parameters located approximately 179 km from the village of Karangkandri. The black box outlines the megathrust source area of the Indo-Australian Subduction Zone. The red lines and red boxes indicate the segmentation of the megathrust earthquake source used in the numerical simulation. The colour gradient from red to blue is generated from the tsunami generation model, where this gradient indicates the initial tsunami height due to seafloor deformation on the Central Java Thrust segment as the tsunami generation source.

This phenomenon indicates that significant seafloor deformation due to megathrust activity can generate initial tsunami wave heights that vary along the subduction zone. The initial wave height is then influenced by factors such as sea depth, seafloor topography, and the distance from the earthquake source to the coastline (Ridwan et al., 2023. Therefore, a deep understanding of earthquake source parameters and tsunami wave propagation characteristics is crucial for mitigating disaster risks in coastal areas of Cilacap, particularly in Karangkandri Village.

Table 3 Sources of Tsunami generation in Karangkandri.

Epicenter (Deg)		Dimension (km)		Focal Depth (km)
Lon	Lat	Length	Width	
103.993	7.403	141	91	14
105.075	7.910	141	91	1
106.176	8.614	141	91	18

Focal Mechanism Strike Angle	Dislocation Dip Angle	Dislocation Rake Angle	Dislocation	Mag (Mw)
296	11	90	22	
300	17	90	23	
298	15	90	22	

Source: Numerical analysis results, 2023

The high-resolution grid from LiDAR surveys in this tsunami numerical simulation is focused on Karangkandri Village, achieving a simulation accuracy of 5 x 5 meters. The modelling process for Karangkandri Village involves creating four domains: Domain 1 has a 1,250-meter grid, Domain 2 has a 250-meter grid, Domain 3 has a

50-meter grid, and Domain 4 has a 10-meter grid. The grid design for each domain can be seen in **Figure 5.**

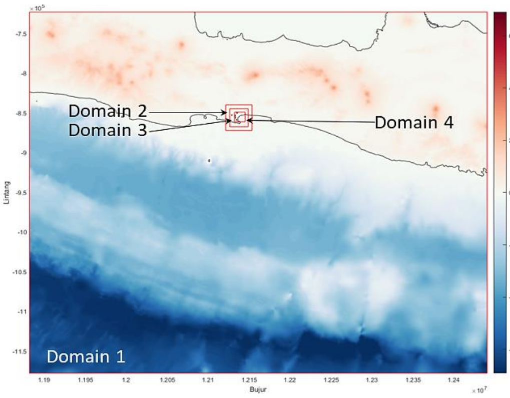

Source: Analysis results, 2023

Figure 3. Design of model and nested grid for numerical simulation of Tsunami in Karangkandri Village.

Numerical Simulation of Tsunami Propagation produces a two-dimensional animation representing the process of tsunami propagation from the tsunami generation source location. The results of the numerical simulation of tsunami propagation are shown in **Figure 6**.

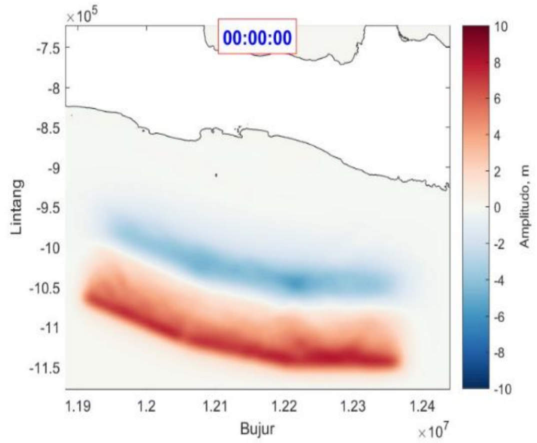

a. Minute 0

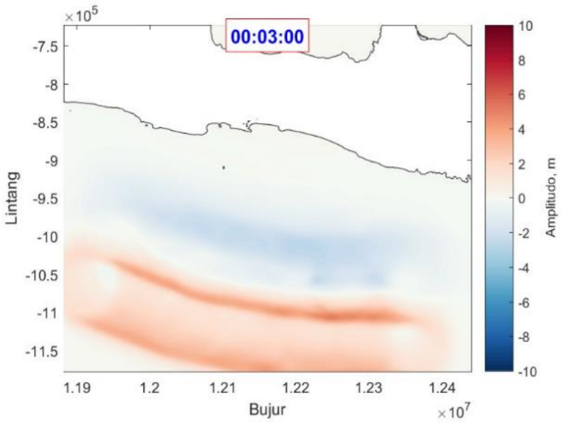

b. Minute 3

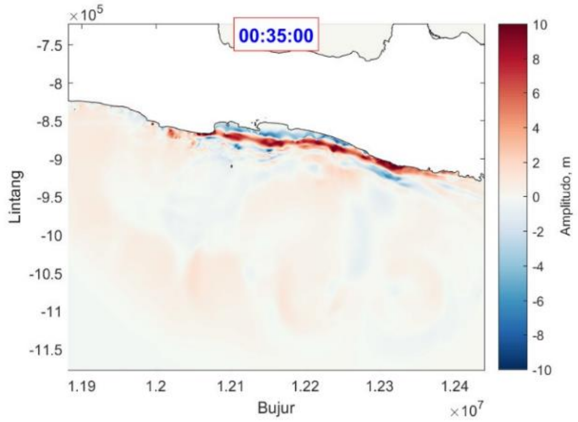

c. Minute 35

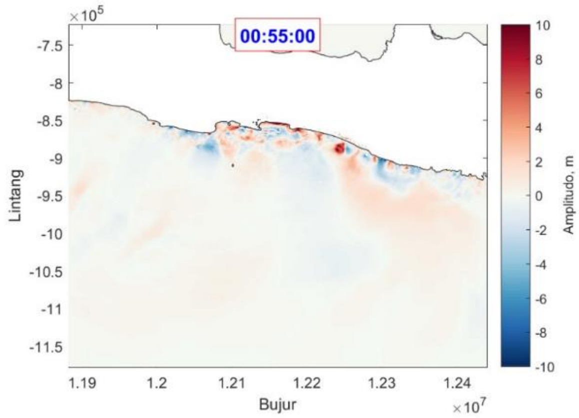

d. Minute 55

Source: Numerical simulation results, 2023

Figure 4. Numerical simulation of Tsunami propagation.

The tsunami propagation affecting Karangkandri Village can be observed in the modelling results shown in **Figure 7**. Based on the simulation snapshot in domain 6, it can be observed that by minute 50, a seawater recession condition occurs around Karangkandri Village. By minute 55, the tsunami had already reached the southern part of Karangkandri Village, and it continued to inundate the land in Karangkandri Village. By minutes 60 and 65, waves had begun to flood the southern part of Karangkandri Village, which included residential areas and the industrial area of the Cilacap Power Plant.

The tsunami heights at measurement points (virtual tide gauges) were recorded based on the simulation results. The measurement point used for Karangkandri Village is located around the Karangkandri Power Plant. The propagation of the tsunami from the modelling results can be seen through the virtual tide gauge records shown in the tsunami's height and arrival time graph at Karangkandri Village. According to the graph in **Figure 8**, the tsunami arrives at the Karangkandri Power Plant measurement point at minute 54, reaching a maximum height of 7.34 meters. Additionally, it can be observed that a phenomenon of low tide precedes the tsunami. After this highest wave, subsequent wave heights decrease over time (**Figure 7**).

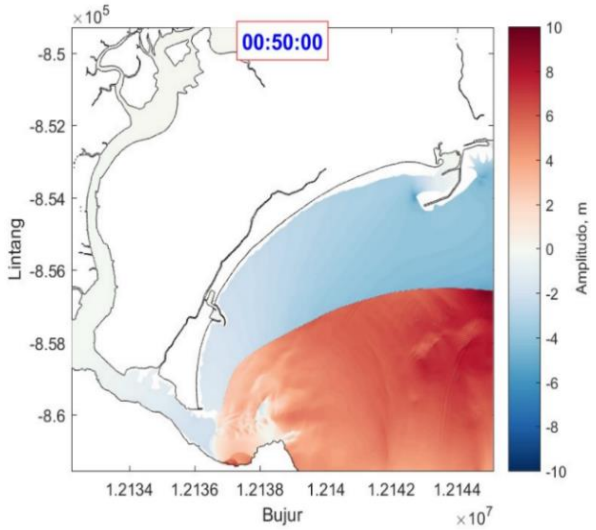

a. Propagation at minute 50

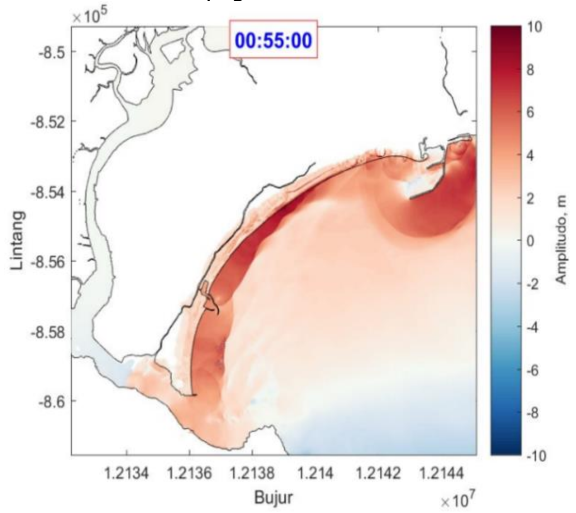

b. Propagation at minute 55

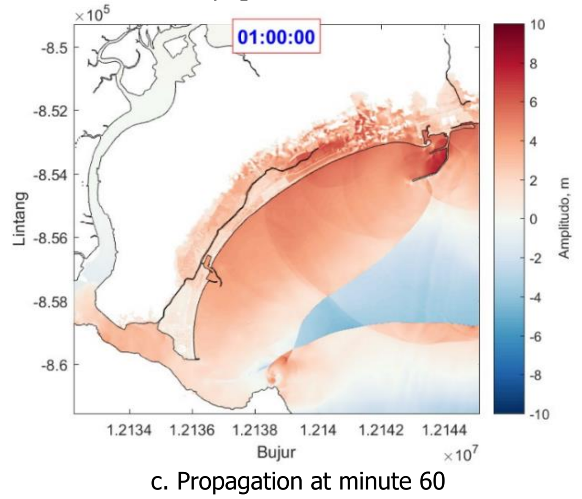

c. Propagation at minute 60

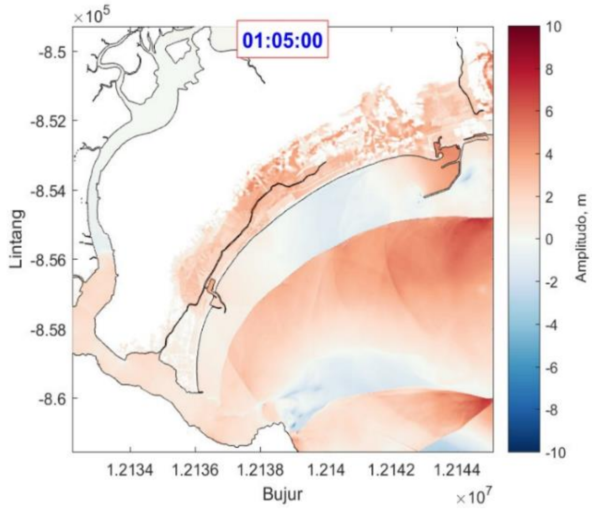

b. Propagation at minute 65

Figure 5. Numerical Simulation of Tsunami propagation.

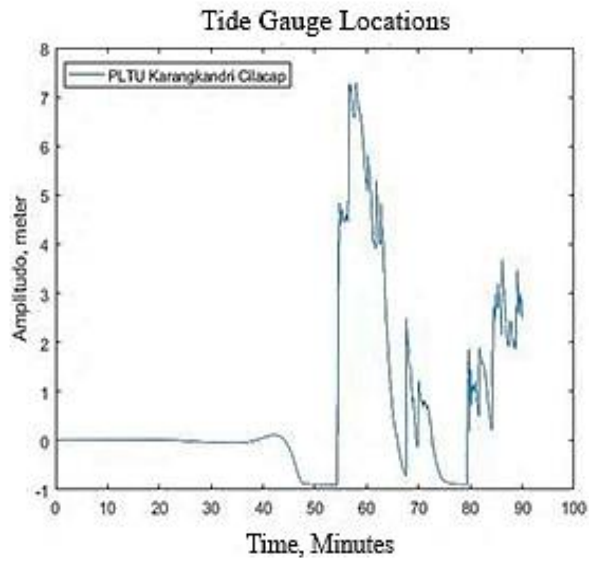

a. Tsunami Height and Arrival Time Graph

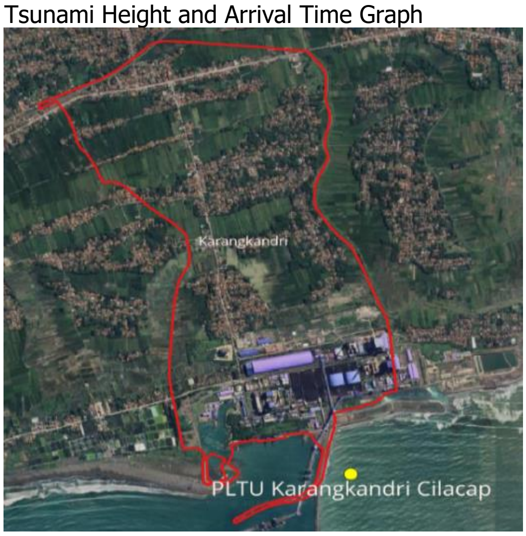

b. Tsunami Measurement Point Location

Source: Numerical model processing results, 2023

Figure 6. (a) Tsunami height and arrival time graph, (b)Tsunami measurement point location.

Based on the calculation of tsunami inundation depth using the roughness coefficient, the inundation depth that affected Karangkandri Village can be determined and subsequently used to create a tsunami inundation map with a maximum height of 9.6 meters. According to the calculation results, the total area of tsunami inundation covers 416.11 hectares, reaching a distance of 1.6 km from the coastline of Karangkandri Village (**Figure 9**).

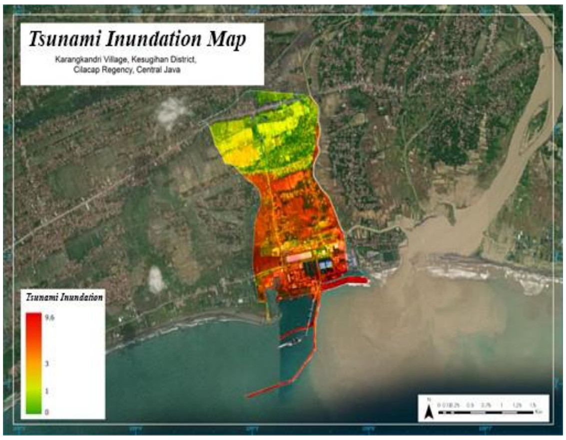

Source: Numerical simulation results, 2023
Figure 7 Tsunami inundation map of Karangkandri Village.

Hazard Index

Based on the high inundation range and hazard index classification above, the affected land area in Karangkandri Village is classified into three hazard index categories: a high hazard index covering an area of 105.48 hectares, a medium hazard index covering 143.89 hectares, and a low hazard index covering 136.89 hectares. Additionally, the non-hazardous area spans 34.3 hectares (**Figure 10**). Therefore, the total tsunami hazard-affected area in Karangkandri Village is approximately 386.25 hectares, which is about 92.8% of the village's total area of 420.55 hectares, with a medium hazard index.

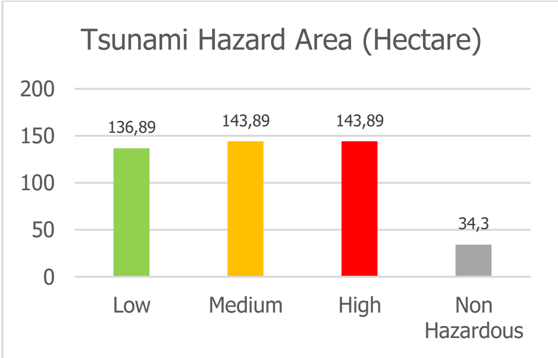

Source: Analysis results, 2023
Figure 8. Extent of Tsunami hazard classes in Karangkandri Village.

Meanwhile, the hazard classes can be seen in the tsunami hazard map of Karangkandri Village (**Figure 11**). From the map, it can be seen that almost half of the southern area of Karangkandri Village is affected and traversed by tsunami waves, namely in fishermen's settlements and areas near the Steam Power Plant (PLTU) of Karangkandri Beach, which is directly adjacent to the coast. This factor is due to the relatively flat and low-lying topography of Karangkandri Village along the southern coastline, with an elevation of 5 meters above sea level and close to the maximum wave height of 9.6 meters. In contrast, the northern part of Karangkandri Village still experiences a relatively low hazard class, with inundation heights of less than 1 meter.

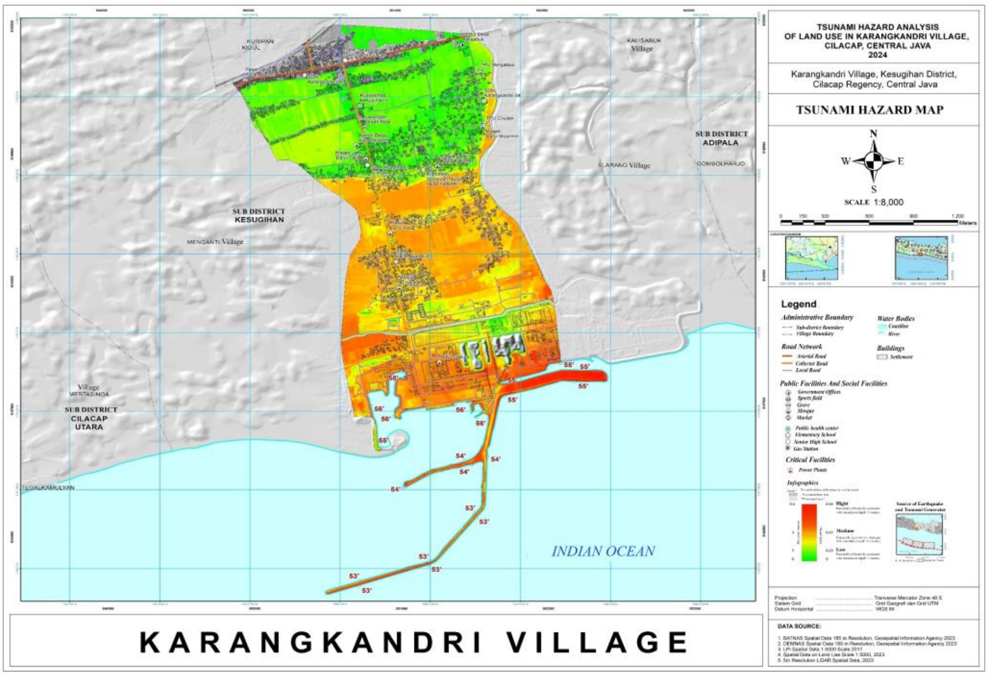

Source: Analysis results, 2023
Figure 9. Tsunami hazard map of Karangkandri Village.

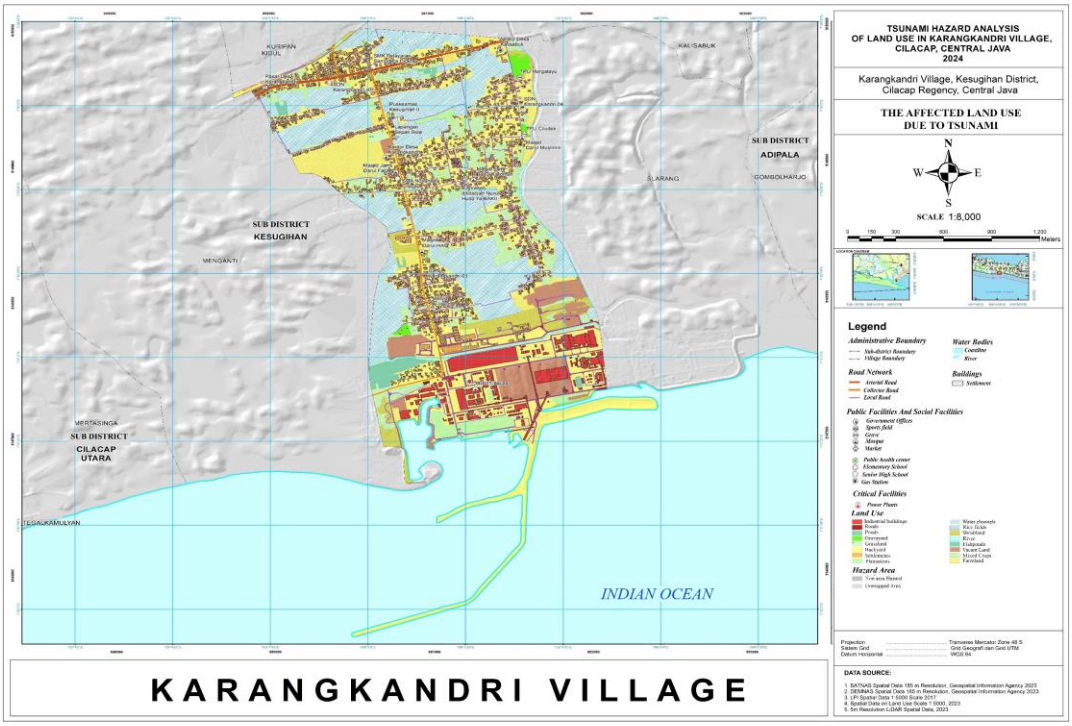

Source: Analysis results, 2023

Figure 10 Land use affected by Tsunami hazard in Karangkandri Village.

The analysis shows that all land use types in Karangkandri Village are affected by tsunami inundation. The built-up land use types affected by tsunami inundation include settlements, industrial buildings, and roads, totalling 1,047 buildings. Meanwhile, non-built-up land cover types include ponds, yards, plantations, rice fields, shrubs, rivers, fish ponds, vacant land, and mixed crops. The total area affected by tsunami inundation is 416.11 hectares. Based on the affected land use map (**Figure 11**), the area of affected land use types in low, medium, and high hazard classes can be calculated as shown in Table 4. Sequentially, the most significantly affected land cover types include yards, with an area of 127.59 hectares (30.34%) and rice fields, with an area of 101.87 hectares (24.22%). Meanwhile, the affected residential land use recorded in the low, medium, and high hazard classes is 41.88 hectares (9.96%), a total of 383 residents are located in the medium hazard index zone, while 3,561 residents are situated in the high hazard index zone. The high hazard index indicates a significant population exposure, which is primarily influenced by the dense residential settlements in the coastal area.

The proximity of these settlements to the shoreline exacerbates the vulnerability of the population to potential tsunami impacts. Meanwhile, the number of buildings affected by tsunami hazards is 259 in the low-hazard zone, 655 in the medium-hazard zone, and 133 in the high-hazard zone. In comparison, the built-up land in industrial buildings affected is 18.34 hectares or 4.3% of the total area, including the Cilacap Power Plant, one of Indonesia's largest power plants, providing a positive economic impact, including job opportunities and local economic growth. Other land use categories such as ponds, cemeteries, shrubs, fish ponds, and dry fields also experienced impacts, although in smaller percentages than the main categories. The potential physical damage losses to buildings due to tsunami exposure amount to 24.31 billion rupiahs.

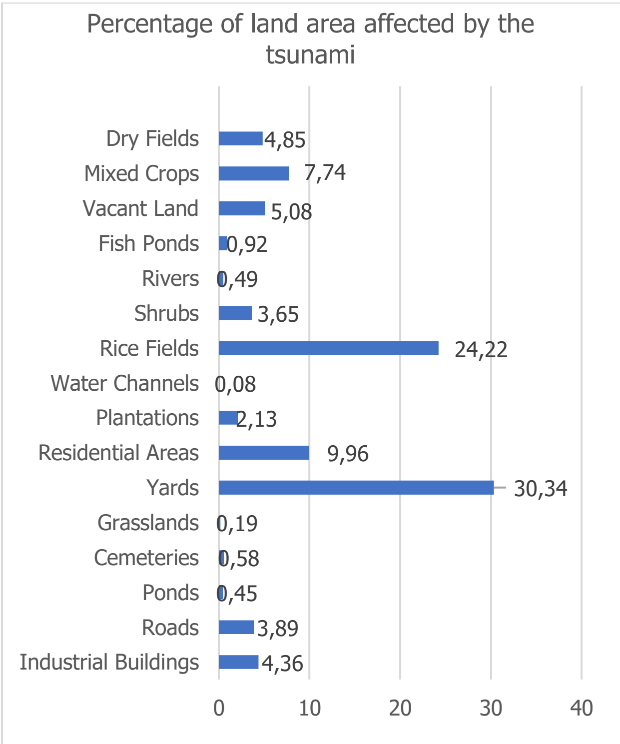

Source: Analysis Results, 2023

Figure 11. Percentage of land area affected by the tsunami.

Table 4 Extent of land cover affected by Tsunami in Karangkandri Village.

Land Use	Hazard Class (Hectares)			Total (hectares)	%
	Low	Medium	Hight		
Industrial Buildings	0,80	1,54	16,00	18,34	4,36
Roads	1,92	2,55	11,91	16,37	3,89
Ponds	-	0,07	1,83	1,90	0,45
Cemeteries	-	0,66	1,79	2,45	0,58
Grasslands	0,05	-	0,76	0,81	0,19
Yards	4,45	30,11	93,04	127,59	30,34
Residential Areas	3,51	13,46	24,91	41,88	9,96
Plantations	-	0,52	8,43	8,95	2,13
Water Channels	-	0,30	0,03	0,34	0,08
Rice Fields	-	3,73	98,15	101,87	24,22
Shrubs	0,08	0,50	14,78	15,35	3,65
Rivers	-	-	2,07	2,07	0,49
Fish Ponds	-	-	3,88	3,88	0,92
Vacant Land	2,64	1,66	17,06	21,36	5,08
Mixed Crops	0,12	6,10	26,35	32,57	7,74
Dry Fields	0,01	1,35	19,02	20,38	4,85
Total Affected Area	**13,58**	**62,54**	**339,99**	**416,11**	**98,95**
Total Unaffected Area				**4,44**	**1,05**
Total Area				**420,55**	**100,00**

Overall, the data shows that the area is almost entirely affected by hazards at various levels. Yards and rice fields are the most affected land uses and are very important to consider in the area's disaster risk mitigation and management planning. The threat of hazards on land use affected by tsunami waves can result in economic losses, physical infrastructure damage, environmental losses (Meilianda et al., 2019). Therefore, mitigation efforts must be made to increase the population's capacity to prepare for tsunami hazards (Imamura et al., 2019).

Land use, especially in built-up areas, can be adapted to mitigation measures such as impermeable structures designed to withstand or sustain harmless damage in the event of a tsunami. These structures can be retaining walls, dikes or other breakwater structures (Sajan et al., 2023, 2024). In addition, tsunamis passing through mangrove forests and coastal buildings are expected to be minimised by collaborating with other non-structural mitigation measures such as community capacity building, improvement of mitigation infrastructure such as signage, temporary evacuation sites, evacuation routes, and optimisation of early warning systems (Lomonaco Et Al., 2023; Shalih Et Al., 2020; Van Balen Et Al., 2024b).

Karangkandri Village can also optimize all tsunami early warning reception modes owned by the District Disaster Management Agency (BPBD) (SMS, email, fax), which can be connected to the Meteorology, Climatology, and Geophysics Agency (BMKG) as a backup. They are optimizing all communication modes among village residents as early warning and evacuation signs such as HT (Handy Talky), *kentongan* (traditional bamboo or wooden slit drum), and mosque speakers.

CONCLUSIONS

Karangkandri Village is located on the southern coast of Java Island, an area prone to tsunamis. Additionally, this village is very close to the Indo-Australian subduction zone. Research results based on numerical modelling indicate that the tsunami propagation starts inundating the southern part of Karangkandri Village, which includes residential areas and the Cilacap PLTU industrial area, from the 60 th to the 65 th minute. At the measurement point in the Karangkandri PLTU, the maximum wave height reached 7.34 meters at the 54th minute. From the tsunami hazard class mapping using the fuzzy tsunami method, Karangkandri Village is dominated by a high hazard class, covering an area of 339.99 hectares, with a total tsunami-affected area of 416.11 hectares. The types of land use extensively affected include yards covering an area of 127.59 hectares (30.34%) and rice fields covering 101.87 hectares (24.22%). The affected residential area covers 41.88 hectares with 1,047 buildings. The government, through stakeholders such as the National Disaster Management Agency (BNPB) and the Meteorology, Climatology, and Geophysics Agency (BMKG), must provide advanced systems utilizing high-end technology to ensure seamless integration with real-time data from earthquake sensors and tsunami detection instruments. When a significant seismic event with tsunami potential is detected, the sirens will automatically activate to alert the public as quickly as possible. However, in certain cases, the sirens can also be manually activated by local authorities or regional disaster management agencies. Additionally, the government should prepare temporary evacuation sites and develop educational programs to enhance public knowledge and awareness of tsunami mitigation measures.

REFERENCES

Aljber, M., Lee, H. S., Jeong, J.-S., & Cabrera, J. S. (2024). Tsunami Inundation Modelling in a Built-In Coastal Environment with Adaptive Mesh Refinement: The Onagawa Benchmark Test. Journal of Marine Science and Engineering, 12(1), 177. https://doi.org/10.3390/jmse12010177

Amri, A., Bird, D. K., Ronan, K., Haynes, K., & Towers, B. (2017). Disaster risk reduction education in Indonesia: challenges and recommendations for scaling up. Natural Hazards and Earth System Sciences, 17(4), 595–612. https://doi.org/10.5194/nhess-17-595-2017

ARANGUIZ, R.; RAMOS, M.; SEPÚLVEDA, I.; VILLAGRA, P. A new generation of tsunami inundation maps of Chilean cities: tsunami source database and probabilistic hazard analysis. *Coastal Engineering Journal*, v. 66, n. 2, p. 361–379, 2024. Disponível em: https://doi.org/10.1080/21664250.2024.2326269. Berryman, K. (2006). Review of Tsunami Hazard and Risk in New Zealand.

BMKG. (2024). *Katalog Tsunami Indonesia Tahun 416-2023.*

BNPB. (2018). *Modul Teknis Penyusunan Kajian Risiko Bencana Tsunami*. Direktorat Pengurangan Risiko Bencana BNPB.

BNPB. (2023). *RBI RISIKO BENCANA INDONESIA BNPB "Memahami Risiko Sistemik di Indonesia."*

Badan Pusat Statistik. (2023). *Kecamatan Kesugihan Dalam Angka Kesugihan Subdistrict In Figures 2023*. https://cilacapkab.bps.go.id/publication/downloa

Briseid Storrøsten, E., Ragu Ramalingam, N., Lorito, S., Volpe, M., Sánchez-Linares, C., Løvholt, F., & Gibbons, S. J. (2024). Machine learning emulation of high resolution inundation maps. Geophysical Journal International, 238(1), 382–399. https://doi.org/10.1093/gji/ggae151

Chen, C., Peng, C., Nandasena, N. A. K., & Yan, H. (2024). Experimental investigation on tsunami impact reduction on a building by a Mangrove forest. Estuarine, Coastal and Shelf Science, 301, 108756. https://doi.org/10.1016/j.ecss.2024.108756

Crescenzo, L., Guthrie, R., & Calvello, M. (2024). Evaluating the performance of propagation models of flow-like landslides at regional scale. *Landslides, 21(2),* 229–243. https://doi.org/10.1007/s10346-023-02162-z

Handoyo, G., Sutoyo, S., & Syafiudin, M. F. (2023). Analisis Risiko dan Strategi Mitigasi Bencana Tsunami Di Pesisir Selatan Jawa Studi Kasus : Kabupaten Cilacap. Jurnal Teknik Sipil Dan Lingkungan. https://api.semanticscholar.org/CorpusID:261485644

Hayashi, K., Marchuk, An. G., & Vazhenin, A. P. (2018). Generating Boundary Conditions for the Calculation of Tsunami Propagation on Nested Grids. Numerical Analysis and Applications, 11(3), 256–267. https://doi.org/10.1134/S1995423918030060

Imamura, F., Boret, S. P., Suppasri, A., & Muhari, A. (2019). Recent occurrences of serious tsunami damage and the future challenges of tsunami disaster risk reduction. *Progress in Disaster Science*, 1, 100009. https://doi.org/10.1016/j.pdisas.2019.100009

Koshimura, S., Adriano, B., Mizutani, A., Mas, E., Ohta, Y., Nagata, S., Takeda, Y., Vescovo, R., Wiguna, S., Abe, T., & Suzuki, T. (2024). *The 2004 Noto Peninsula Earthquake Tsunami-It's Generation, Propagation, Inundation, and Impact.* https://doi.org/10.5194/egusphere-egu24-22527

Law, J., & Pangka, K. (2014). Medical and humanitarian relief post-2004 Indian Ocean tsunami. University of Western Ontario Medical Journal, 83(2), 23–25. https://doi.org/10.5206/uwomj.v83i2.4437

Lomonaco, P., Mitchell, W., Kelty, K., Cox, D., & Tomiczek, T. (2023). LARGE SCALE LABORATORY OBSERVATIONS OF WAVE FORCE REDUCTION ON COASTAL BUILDINGS BY AN IDEALIZED MANGROVE FOREST. Coastal Engineering Proceedings, 37, 87. https://doi.org/10.9753/icce.v37.structures.87

Matsutomi, H., & Arikawa, T. (2023). Tsunami Run-Up Considering Time Variation Of Density Of Inundation Water. Coastal Engineering Proceedings, 37, 2. https://doi.org/10.9753/icce.v37.papers.2

Meilianda, E., Pradhan, B., Syamsidik, Comfort, L. K., Alfian, D., Juanda, R., Syahreza, S., & Munadi, K. (2019). Assessment of post-tsunami disaster land use/land cover change and potential impact of future sea-level rise to low-lying coastal areas: A case study of Banda Aceh coast of Indonesia. International Journal of Disaster Risk Reduction, 41, 101292. https://doi.org/10.1016/j.ijdrr.2019.101292

Prasetyo, W. E., Irawan, L. Y., Hartono, R., & Santosa, E. B. (2023). Seismic hazard analysis using Deterministic Seismic Hazard Analysis (DSHA) Method: A case study in Southern Malang District, East Java. *Jurnal Pendidikan Geografi: Kajian, Teori, Dan Praktek Dalam Bidang Pendidikan Dan Ilmu Geografi, 28*(2), 209. https://doi.org/10.17977/um017v28i22023p209-227

Pemerintah Kabupaten Cilacap. (2021). *Peraturan Daerah Kabupaten Cilacap Nomor 1 Tahun 2021 Tentang Perubahan Atas Peraturan Daerah Kabupaten Cilacap Nomor 9 Tahun 2011 Tentang Rencana Tata Ruang Wilayah Kabupaten Cilacap Tahun 2011-2031*. https://peraturan.bpk.go.id/Details/170971/perda-kab-cilacap-no-1-tahun-2021

PuSGeN. (2017). *Peta Sumber dan Bahaya Gempa Indonesia 2017*. Balitbang Kementerian PUPR

Ridwan, M., Soehaimi, A., Sinung Baskoro, S. R., Sopian, Y., Setianegara, R., & Cita, A. (2023). Pengembangan Peta Bahaya Gempabumi di Batuan Dasar untuk Daerah Cilacap dan Sekitarnya. Jurnal Geologi Dan Sumberdaya Mineral, 24(1), 31–38. https://doi.org/10.33332/jgsm.geologi.v24i1.704

Sabah, N., & Sil, A. (2023). A comprehensive report on the 28th September 2018 Indonesian Tsunami along with its causes. Natural Hazards Research, 3(3), 474–486. https://doi.org/10.1016/j.nhres.2023.06.003

Sajan, M. K., Chaudhary, B., Akarsh, P. K., & Kumar, S. (2023). Investigating the impact of tsunami waves on gabion material-reinforced coastal structures: A

numerical analysis. Materials Today: Proceedings. https://doi.org/10.1016/j.matpr.2023.09.033
Sajan, M. K., Chaudhary, B., Akarsh, P. K., & Kumar, S. (2024). Geosynthetic reinforced rubble mound breakwater for mitigation of tsunami-induced damage. Geotextiles and Geomembranes, 52(1), 72–94. https://doi.org/10.1016/j.geotexmem.2023.09.003
Setyaningsih, D. P., Sutiono, H. E. C. P., Paramanandi, A. R. G., Khasanah, E. U., Wahyuni, T., Jati, B. A. E. K., Akbar, M. F. Al, Widyatmanti, W., & Wibowo, T. W. (2023). TSUNAMI HAZARD Modeling In The Coastal Area Of Kulon Progo Regency. International Journal of Remote Sensing and Earth Sciences (IJReSES), 19(2), 184. https://doi.org/10.30536/j.ijreses.2022.v19.a3822
Shalih, O., Setiadi, H., Nurlambang, T., & Sumadio, W. (2020). Toward a community resilience framework for disaster risk management. a case study: Landslide Cisolok in Sukabumi 2018 and Sunda strait tsunami in Pandeglang 2018. E3S Web of Conferences, 156. https://doi.org/10.1051/e3sconf/202015601011
Van Balen, I., Cels, J., Adams, K., Baiguera, M., Rossetto, T., Antonini, A., Wüthrich, D., Istrati, D., Buldakov, E., Chandler, I., & Mcgovern, D. (2024a). Tsunami Runup Attenuation By Onshore Obstacles. CoastLab 2024: Physical Modelling in Coastal Engineering and Science. https://doi.org/10.59490/coastlab.2024.763
Xiaoming Wang, & Liu. (2009). User Manual For Comcot Version 1.7 (First Draft).
Yamazaki, Y., Cheung, K. F., & Kowalik, Z. (2011). Depth-integrated, non-hydrostatic model with grid nesting for tsunami generation, propagation, and run-up. International Journal for Numerical Methods in Fluids, 67(12), 2081–2107. https://doi.org/10.1002/fld.2485
Yusup, Y., Tjahjono, G. A., & Sholeh, S. (2023). Impact of tourism gentrification on Megathrust Disaster Risk in Pacitan Regency. IOP Conference Series: Earth and Environmental Science, 1190(1), 012035. https://doi.org/10.1088/1755-1315/1190/1/012035
Zuliansah, A. B. R., Windujati, U., Rasyif, T. M., Mahlil, T., & Januriyadi, N. F. (2023). Performance Evaluation of DualSPHysics and COMCOT Programs through Numerical Testing for Simulating Tsunami Propagation and Overtopping on Seawalls. E3S Web of Conferences, 447, 01014. https://doi.org/10.1051/e3sconf/202344701014